MOL PHARM

MOLECULAR PHARMACOLOGY

A Peptide Accelerating the Conversion of Plasminogen Activator Inhibitor-1 to an Inactive Latent State

Lisa Mathiasen, Daniel M. Dupont, Anni Christensen, Grant E. Blouse, Jan K. Jensen, Ann Gils, Paul J. Declerck, Troels Wind, and Peter A. Andreasen

Department of Molecular Biology, Aarhus University, Denmark (L.M., D.M.D., A.C., G.E.B., J.K.J., T.W., P.A.A.); and Laboratory for Pharmaceutical Biology, Faculty of Pharmaceutical Sciences, Katholieke Universiteit, Leuven, Belgium (A.G., P.J.D.)

ABSTRACT

The serpin plasminogen activator inhibitor-1 (PAI-1) is a specific inhibitor of plasminogen activators and a potential therapeutic target in cancer and cardiovascular diseases. Accordingly, formation of a basis for development of specific PAI-1-inactivating agents is of great interest. One possible inactivation mode for PAI-1 is conversion to the inactive, so-called latent state. We have now screened a phage-displayed peptide library with PAI-1 as bait and isolated a 31-residue cysteine-rich peptide that will be referred to as paionin-4. A recombinant protein consisting of paionin-4 fused to domains 1 and 2 of the phage coat protein g3p caused a 2- to 3-fold increase in the rate of spontaneous inactivation of PAI-1. Paionin-4-D1D2 bound PAI-1 with a K_D in the high nanomolar range. Using several biochemical and biophysical methods, we demonstrate that paionin-4-D1D2-stimulated inactivation consists of an acceleration of conversion to the latent state. As demonstrated by site-directed mutagenesis and competition with other PAI-1 ligands, the binding site for paionin-4 was localized in the loop between α-helix D and β-strand 2A. We also demonstrate that a latency-inducing monoclonal antibody has an overlapping, but not identical binding site, and accelerates latency transition by another mechanism. Our results show that paionin-4 inactivates PAI-1 by a mechanism clearly different from other peptides, small organochemical compounds, or antibodies, whether they cause inactivation by stimulating latency transition or by other mechanisms, and that the loop between α-helix D and β-strand 2A can be a target for PAI-1 inactivation by different types of compounds.

Plasminogen activator inhibitor type-1 (PAI-1) is a fast and specific inhibitor of the urokinase-type plasminogen activator (uPA) and the tissue-type plasminogen activator. PAI-1 is therefore an important regulator of the physiological and pathophysiological functions of plasminogen activation. A high level of PAI-1 in blood is associated with an increased risk of thrombotic events (for review, see Vaughan, 1998). PAI-1 is therefore a potential target for antithrombotic therapy. A high level of PAI-1 in tumors is associated with a poor prognosis, and several studies have suggested that PAI-1 is

contributory to tumor invasion and metastasis (for review, see Andreasen et al., 1997, 2000; Durand et al., 2004; Andreasen, 2007). PAI-1 is therefore a potential target for anticancer therapy.

PAI-1 belongs to the serpins, a protein family of which the best characterized members are known to be inhibitors of serine proteases. Serpins are globular proteins consisting of three β-sheets (A, B, and C) and nine α-helices (A–I). Of crucial importance for the inhibitory mechanism of serpins is the surface-exposed reactive center loop (RCL), tethered between β-strands 1C and 5A. The active site of the protease attacks the P1-P1′ bond in the RCL as a substrate, but at the enzyme-acyl intermediate stage, where the active site serine of the protease and the P1 residue are linked by an ester bond, the N-terminal part of the RCL inserts as β-strand 4, thereby pulling the protease to the opposite pole of the serpin and distorting its active site. The energy required for this

aspet

ABBREVIATIONS: PAI, plasminogen activator inhibitor; uPA, urokinase-type plasminogen activator; RCL, reactive center loop; HBS, HEPES-buffered saline; mAb, monoclonal antibody; HRP, horseradish peroxidase; bis-ANS, 4,4′-dianilino-1,1′-bisnaphthyl-5,5′-disulfonic acid, dipotassium salt; XR5118, (3Z,6Z)-6-benzylidene-3-(2-dimethylaminoethyl-thio)-2-(thienyl)methylene-2,5-piperazinedione hydrochloride.; ELISA, enzyme-linked immunosorbent assay; FPLC, fast protein liquid chromatography; D1D2, domain 1 and 2; S-2444, pyroGlu-Gly-Arg-*p*-nitroanilide; PAGE, polyacrylamide gel electrophoresis; IANBD, *N*-((2-(iodoacetoxy)ethyl)-*N*-methyl)-amino-7-nitrobenz-2-oxa-1,3-diazole; wt, wild type.

process stems from stabilization of the serpin in the relaxed conformation with an inserted RCL, as opposed to the stressed conformation with a surface exposed RCL (for reviews, see Andreasen et al., 1997, 2000; Wind et al., 2002; Durand et al., 2004; Huntington, 2006; Andreasen, 2007).

Apart from its interaction with serine proteases, PAI-1 also binds with high affinity to the blood plasma and extracellular matrix protein vitronectin. The complexes of PAI-1 with its target proteases bind with high affinity to some endocytosis receptors of the low-density lipoprotein family (for reviews, see Andreasen et al., 1997, 2000; Wind et al., 2002; Durand et al., 2004; Huntington, 2006; Andreasen, 2007).

PAI-1 and antithrombin III are the only serpins known to spontaneously adopt the relaxed conformation without prior cleavage of the RCL. This transition is referred to as latency transition and involves the insertion of the N-terminal part of the intact RCL as β-strand 4A, whereas the C-terminal part and β-strand 1C is stretched out on the surface of the molecule (for reviews, see Andreasen et al., 1997, 2000; Wind et al., 2002; Durand et al., 2004; Huntington, 2006; Andreasen, 2007).

Attempts to use PAI-1 as a therapeutic target should be based on the knowledge of its inhibitory mechanism. There are several possible ways of inactivating the antiproteolytic actions of PAI-1. Several well studied examples include 1) introducing a steric hindrance that blocks the initial complex formation between PAI-1 and its target proteases; 2) an inhibition of the conformational change in PAI-1 that is associated with complex formation, resulting in cleavage of PAI-1 as a substrate; and 3) conversion of PAI-1 to an inactive (e.g., latent) form or polymerized form. Several antibodies have been described that inactivate PAI-1 by these different methods (for review, see Gils and Declerck, 2004). For instance, the monoclonal antibody MA33B8 was demonstrated to increase strongly the rate of latency transition of PAI-1. The fact that MA33B8 binds preferentially to RCL-inserted forms of PAI-1 prompted the hypothesis that antibody binding depends on a partial insertion of the RCL in active PAI-1, and that this partial insertion results in exposure of the epitope that permits binding of MA33B8 and the subsequent increase in the rate of latency transition (Verhamme et al., 1999). The epitope for MA33B8 includes residues from the loop connecting α-helix D and β-strand 2A, from β-strand 3A, and from β-strand 2B (Gorlatova et al., 2003; Naessens et al., 2003). Other PAI-1 inactivators, including various peptides corresponding to the reactive center loop in PAI-1, have been found to be able to insert between β-strands 3A and 5A, inhibit RCL insertion during reaction with target proteases, and thus induce substrate behavior (Eitzman et al., 1995; Xue et al., 1998). A number of organo-chemical compounds were reported to inactivate the antiproteolytic activity of PAI-1 by a variety of mechanisms (for reviews, see Durand et al., 2004; Andreasen, 2007; Stoppelli et al., 2008). High concentrations of nonionic detergents were found to induce substrate behavior and then latency transition (Ehnebom et al., 1997; Gils and Declerck, 1998; Andreasen et al., 1999; Gils et al., 2000, 2003). Some other compounds inactivated PAI-1 by less characterized mechanisms (Gårdsvoll et al., 1998; Chikanishi et al., 1999; Neve et al., 1999).

From a phage-displayed peptide library, we have now isolated a PAI-1 binding peptide motif that causes a considerable increase in the rate of latency transition. We have demonstrated that the peptide binds in an area overlapping with the epitope for MA33B8 and another latency-inducing antibody, Mab-7. Although the peptide seemed to increase the rate of latency transition by a mechanism different from that of the antibodies, our findings show that a latency inducing activity can reside in a molecule much smaller than an antibody. This peptide sequence may provide a basis for specific and high-affinity PAI-1-neutralizing agents after proper affinity maturation.

Materials and Methods

PAI-1. Human PAI-1, murine PAI-1, the murine-hF-human chimera, human-hF-murine PAI-1 chimera, and variants of PAI-1 carrying one or more mutations were expressed with an N-terminal His$_6$-tag and purified from *Escherichia coli* cells as described previously (Wind et al., 2003; Dupont et al., 2006). The murine-hF-human chimera consisted of the murine sequence from the N terminus to residue 122, the conserved human and murine sequence between residues 123 and 142, and the human sequence from residue 143 to the C terminus. Likewise, the human-hF-murine chimera consisted of the human sequence from the N terminus to residue 122, the conserved murine and human sequence between residues 123 and 142, and the murine sequence from residue 143 to the C terminus. Natural glycosylated human PAI-1 was purified in the latent form by immunoaffinity chromatography from serum-free conditioned medium of dexamethasone-treated HT-1080 cells and reactivated by denaturation with 4 M guanidinium chloride and dialysis against HEPES-buffered saline (HBS; 10 mM HEPES, pH 7.4, and 140 mM NaCl) (Munch et al., 1993). In some cases, preparations of recombinant PAI-1 with ~100% activity were generated by hydrophobic chromatography using phenyl-Sepharose and an ammonium sulfate gradient, followed by concentration on a small column of heparin-Sepharose (Kvassman and Shore, 1995). Labeling of the S340C (P9) residue of PAI-1 was performed with *N*-((2-(iodoacetoxy)ethyl)-*N*-methyl)amino-7-nitrobenz-2-oxa-1,3-diazole (IANBD ester; Invitrogen, Carlsbad, CA) to create the fluorescently labeled variant, PAI-1$_{P9-NBD}$, essentially as described previously (Shore et al., 1995).

Proteases. Natural human uPA was purchased from Wakamoto Pharmaceutical Co. (Tokyo, Japan). Low-molecular-weight uPA (i.e., uPA N-terminally truncated at Lys136), was prepared as described previously (Egelund et al., 2001b).

Antibodies. Monoclonal anti-PAI-1 antibodies (mAbs) were described previously: mAb-1 (Nielsen et al., 1986; Bødker et al., 2003); mAb-2 (Wind et al., 2001); mAb-5 (Munch et al., 1991); mAb-6 (Wind et al., 2001); mAb-7 (Gils et al., 2003); MA33B8 (Verhamme et al., 1999; Gorlatova et al., 2003; Naessens et al., 2003); MAH4B3 (Declerck et al., 1995; Gils et al., 2003). A preparation of rabbit polyclonal anti-PAI-1 antibodies was described previously (Offersen et al., 2003). A horseradish peroxidase (HRP)-conjugated monoclonal anti-M13 phage antibody was purchased from GE Healthcare (Chalfont St. Giles, Buckinghamshire, UK).

Miscellaneous Materials. XR5118 (Friederich et al., 1997) was a kind gift from Dr. Thomas Frandsen, Finsen Laboratory, Copenhagen, Denmark; bis-ANS was purchased from Molecular Probes; heparin was purchased from Sigma (St. Louis, MO).

Screening of Phage Library. Monoclonal antibodies, mAb-1 and mAb-5 (5 μg/ml in 100 mM NaHCO$_3$/Na$_2$CO$_3$, pH 9.6), were immobilized in Immunotubes (Maxisorp; NUNC A/S, Roskilde, Denmark), and unspecific binding was blocked by HBS supplemented with 5% nonfat dry milk powder. PAI-1 (50 nM in HBS + 20% glycerol), alone or preincubated with 20 μM bis-ANS, 200 μM SDS, 50 μM XR5118, was captured in the antibody-coated tubes followed by incubation with approximately 10^{11} colony-forming units from each of four peptide repertoires in the formats X$_7$, CX$_7$C, CX$_{10}$C, and

CX$_3$CX$_3$CX$_3$C, respectively, where X denotes random natural amino acids (Koivunen et al., 1994). After extensive washing, bound phages were eluted with a glycine/HCl buffer, pH 2.2, and neutralized. The neutralized phages were propagated in *E. coli* TG1 cells and concentrated from the culture supernatant by precipitation with NaCl and polyethylene glycol. Alternating antibodies were used for subsequent rounds of selection (mAb-1 in first, third, and fifth rounds, and mAb-5 in second, fourth, and sixth rounds of selection) to avoid enrichment of antibody-specific phages. After the sixth round of selection, phage was prepared from 64 individual clones, 16 from each of the four different PAI-1 preparations, and tested for binding in an ELISA with mAb-1- or mAb-5-immobilized PAI-1 (see *ELISA for Measuring PAI-1-Paionin-4-Phage Particle Binding*). The sequences of the peptides displayed on individual phage clones were determined by sequencing the encoding DNA as described previously (Wind et al., 2001).

Expression of Paionin-4 Peptide Sequence Fused to the N-Terminal Domains of the Phage Coat Protein g3p. The procedure for cloning and expression of the peptide-containing fusion proteins has been described in detail previously (Hansen et al., 2005). In brief, a DNA fragment encoding the paionin-4 peptide fused to domain 1 and 2 (D1D2) of the minor phage coat protein g3p was amplified from the respective phage using PCR. The generated PCR products were purified and ligated into the *E. coli* expression vector pET20b(+) (Novagen, Nottingham, UK). The inserts and their flanking cloning sites were validated by sequencing and the paionin-4-D1D2 fusion protein was expressed from *E. coli* BL21(DE3)pLysS cells (Novagen) and purified using immobilized metal affinity chromatography and size-exclusion chromatography (Scott and Smith, 1990).

DNA fragments encoding deletion mutants of the paionin-4 sequence were PCR-amplified from paionin-4 phages and ligated into a modified pET20b(+) vector, pETD1D2 (Hansen et al., 2005). The resulting vectors allowed the expression of fusion proteins composed of truncated paionin-4 and domains 1 and 2 from the phage coat protein g3p. Expression and purification of these was performed as described above for paionin-D1D2.

ELISA for Measuring PAI-1-Paionin-4-Phage Particle Binding. Five microliters of supernatant from paioin-4 phage-infected *E. coli* cultures, incubated overnight at 37°C to propagate the phage, was mixed with 95 μl of HBS supplemented with 0.25 μg of PAI-1, which had been preincubated with inactivators as described, 5% nonfat dry milk powder, and 20% glycerol and incubated for 1 h at room temperature. Formed PAI-1-phage complexes were captured on 500 ng of monoclonal anti-PAI-1 antibody, mAb1 or mAb5, immobilized in wells of a 96-well Maxisorp plate (Nunc A/S) and detected with an HRP-conjugated monoclonal anti-M13 antibody (Amersham). The ELISA was developed with a peroxidase reaction.

ELISA for Measuring PAI-1-Paionin-3-Phage Particle Binding. *E. coli* PAI-1, ~100% in the active form after phenyl-Sepharose chromatography, in HBS with 0.2% bovine serum albumin and in concentrations as indicated for each single experiment, was incubated for 2 min at room temperature in the absence or presence of 100 nM monoclonal antibody (mAb-33B8, mAb-7, or mAb-5) or at 37°C in the presence of 10 μM paionin-4-D1D2 fusion protein or 10 μM D1D2. Samples were then taken for analysis in an ELISA, in which 500 ng of monoclonal anti-PAI-1 antibody mAb-6 was coated onto the wells of a 96-well Maxisorp plate (Nunc A/S). The PAI-1 samples were added to the wells in a concentration of 10 nM and incubated in the wells for 30 min at room temperature. The next layer was paionin-3 phage [CLTWPRYLC-version (Dupont et al., 2006); ~10^7-10^8 colony-forming units/ml] for 30 min at room temperature. The amount of bound phage was estimated using HRP-conjugated anti-M13 monoclonal antibody (diluted 2000-fold; GE Healthcare) and a peroxidase reaction. To ensure that equal amounts of the PAI-1 variants had been captured at different incubation conditions, a parallel ELISA was performed with 1 μg/ml polyclonal rabbit-anti-PAI-1 antibody instead of paionin-3 phage and with HRP-conjugated

swine-anti-rabbit serum (diluted 2000-fold in HBS-bovine serum albumin; Dako Denmark A/S, Glostrup, Denmark) instead of HRP-conjugated anti-M13 antibody.

ELISA for Mapping of the Binding Site for Paionin-4 by the Use of Monoclonal Antibodies. Maxisorp immunotitre 96-well plates were coated with 500 ng of polyclonal anti-PAI-1 antibody. PAI-1 (0.5 μg/ml) was added and incubated for 1 h. Paionin-4 phage (1 μg/well) and monoclonal antibodies (5 μg/ml) were added simultaneously and allowed to react for 1 h. Phage was detected by addition of HRP-conjugated monoclonal anti-M13 antibody. As a control, monoclonal antibodies, instead of paionin-4 phage, were detected with HRP-conjugated goat anti-mouse antiserum. The ELISA was developed with a peroxidase reaction.

Gel Filtration. Complex formation between PAI-1 and paionin-4-D1D2 and its deletion mutants were analyzed by fast protein liquid chromatography (FPLC) gel filtration on a Superose 12 HR10/30 column (GE Healthcare) in HBS, pH 7.4, 0.5 M NaCl, at 4°C using a flow rate of 0.4 ml/min. The following markers were used: β-galactosidase (M_r 540,000), bovine serum albumin (M_r 67,000), ovalbumin (M_r 43,000), thrombin (M_r 34,000), and chymotrypsin (M_r 25,000).

Fluorescence Emission Spectroscopy. Emission spectra of the binding interactions between labeled PAI-1$_{P9-NBD}$ and fusion proteins or monoclonal antibodies were carried out in a SPEX-3 spectrofluorimeter equipped with a Peltier temperature controller maintaining the measurement and incubation temperatures at 25°C. Fluorescence experiments were carried out using semi-micro (0.2 × 1.0 cm) quartz cuvettes and in a reaction buffer containing 30 mM HEPES, 135 mM NaCl, 1 mM EDTA, 0.1% polyethylene glycol 8000, pH 7.4. The excitation wavelength used for studying the fluorescence of PAI-1$_{P9-NBD}$ was 480 nm, and the emission spectra were scanned from 500 to 650 nm using a bandwidth of 5 and 2.5 nm for the excitation and emission beams, respectively. Emission spectra for PAI-1$_{P9-NBD}$ (50 nM) were recorded before and after the addition of fusion proteins or monoclonal antibodies (500 nM) and incubation at 25°C for time periods indicated for each single experiment. Results are presented as the averaged spectra of three independent acquisitions. All individual emission spectra were collected as averages of three emission scans using a 0.5-s integration over a 1.0-nm step resolution and corrected for background fluorescence in the absence of PAI-1$_{P9-NBD}$ and dilution effects, which were typically less than 2%. Spectra of latent PAI-1$_{P9-NBD}$ (50 nM) were collected as described above.

Stopped-Flow Analysis of P9-NBD Labeled PAI-1 Kinetics. Stopped-flow reactions of PAI-1$_{P9-NBD}$ with mAb-7 were measured on a stopped-flow reaction analyzer (SX.18MV; Applied Photophysics, Leatherhead, Surrey, UK) with a thermostatted syringe chamber. Excitation was at 480 nm, and a filter with a cutoff below 515 nm was used to monitor fluorescence emission. Stopped-flow experiments were carried out under pseudo-first-order conditions as has been described previously (Verhamme et al., 1999), with mAb-7 in excess over the tested PAI-1$_{P9-NBD}$ (0.25–3.3 μN). The rate of the fluorescence increase induced by treating PAI-1$_{P9-NBD}$ with mAb-7 was measured as a function of antibody concentration up to 3.3 μN. The corresponding rate constants were evaluated by nonlinear least-squares fitting of a single exponential to the fluorescence progress curves. The apparent second-order rate constant for antibody binding was subsequently determined from plotting the observed first-order rate constants (k_{obs}) against the concentration of mAb-7.

Surface Plasmon Resonance Measurements of PAI-1-Paionin-4 Binding. The binding between paionin-4-D1D2 and different wt and mutant PAI-1 conformations (e.g., active, latent, and protease-complexed) were studied by surface plasmon resonance, using a BIACORE T100 analytical system equipped with a CM5 sensor chip (BIAcore AB, Uppsala, Sweden). Paionin-4-D1D2 was covalently coupled to the chip to approximately 300 response units, using a concentration of 2.5 μg/ml paionin-4-D1D2 in sodium acetate buffer, pH 4.5. PAI-1 in different conformations was diluted in HBS supplemented with 1 mM EDTA, 0.05% Tween 20, and 0.1% bovine

serum albumin at 25°C to concentrations between 0.03 and 2.0 μM and injected at a flow rate of 30 μl/min. After each cycle, the chip was regenerated with 10 μl of a 10 mM glycine/HCl solution, pH 2.5, 1 M NaCl. In another flow channel on the same chip, D1D2 without peptide was immobilized as control. The number of response units bound to the paionin-4-D1D2 flow channel at each particular time point was corrected for nonspecific binding by subtracting the number of response units bound to the D1D2 flow channel at the same time point. The amount of PAI-1 bound to the chip with only D1D2 always corresponded to less than 1 response unit. The K_D for the binding of PAI-1 to paionin-4-D1D2 was determined from the dependence of the amount of PAI-1 bound at steady state on the PAI-1 concentration, fitting the data to the following equation with the use of the software package SigmaPlot (Systat Software, Inc., San Jose, CA): [PAI-1 bound] = ([paionin-4-D1D2] $\times$ [PAI-1])/(K_D + [PAI-1]).

Surface Plasmon Resonance Measurements of PAI-1-mAb-7 Binding. To determine association and dissociation rate constants and equilibrium dissociation constants for the binding between mAb-7 and different wt and mutant PAI-1 conformations (e.g., active, latent, and protease-complexed), the antibody was immobilized on a CM5 chip to 200 response units. The various PAI-1 variants were injected over the chip in concentrations between 0.2 and 500 nM for 60 s at a flow rate of 30 μl/min, after which time the dissociation was followed for 10 min. After each cycle, the chip was regenerated with 10 μl of a 10 mM glycine/HCl solution, pH 2.5, 0.5 M NaCl. The association rate constants, the dissociation rate constant, and the equilibrium dissociation constants were determined by analyzing the kinetic data by a global fit to a 1:1 binding model with the BIACORE T100 evaluation software.

Determination of PAI-1 Specific Inhibitory Activity. To measure the specific inhibitory activity of PAI-1 (i.e., the fraction of PAI-1 forming a stable complex with its target protease), PAI-1 was serially diluted in HBS with 0.25% gelatin, resulting in PAI-1 concentrations between 0.2 and 400 nM, in a volume of 100 μl at 37°C. An aliquot of 100 μl of 10 nM uPA in HBS with 0.25% gelatin was added to each well, followed by incubation for at least 5 min at 37°C. The remaining uPA activity was determined by incubation with the chromogenic peptidyl anilide substrate S-2444 (Chromogenix AB, Moelndal, Sweden) and measurement of the increase in absorbance at 405 nm. The specific inhibitory activity of PAI-1 was calculated from the amount of PAI-1 that inhibited 50% of the uPA.

Determination of PAI-1 Latency Transition Rate. To measure the time course of latency transition of PAI-1, the specific inhibitory activity was measured after varying time periods of incubation at 37°C at a PAI-1 concentration of 400 nM. The half-life for latency transition was calculated from semilogarithmic plots of the specific inhibitory activity versus time.

Determination of IC_{50} Values for Antibody Inactivation of PAI-1. The effect of the monoclonal antibody mAb-7 on the specific inhibitory activity of different PAI-1 variants was measured by titration of the PAI-1 variants against uPA in a direct peptidyl anilide assay in HBS supplemented with 0.25% gelatin, at varying antibody concentrations. In brief, PAI-1 was serially diluted with buffer at 37°C, corresponding to concentrations between 0.2 and 400 nM in a volume of 50 μl. MA33B8 or mAb-7 was added to each PAI-1 dilution series in volumes of 25 μl and concentrations between 0 and 100 nM and incubated for 20 min at 37°C. uPA was then added in portions of 25 μl to a final concentration of 5 nM. After 5-min incubation, remaining uPA activity was determined by incubation with the chromogenic peptidyl anilide substrate S-2444 (Chromogenix AB) at 37°C until suitable color development, followed by absorbance measurement at 405 nM. The specific inhibitory activity of PAI-1 at each antibody concentration was calculated from the amount of PAI-1 that inhibited 50% of the uPA. The IC_{50} values for the antibody were determined from plots of the specific inhibitory activity of PAI-1 against the antibody concentration, as the antibody concentration reducing the specific inhibitory activity to 50%.

Results

Selection of Paionin-4. For isolating PAI-1 binding peptides, we used a combination of four different phage-displayed random peptide libraries, in the formats X_7, CX_7C, $CX_{10}C$, and $CX_3CX_3CX_3C$, respectively, where X denotes random natural amino acids. The cysteine residues shown are oxidized, resulting in constrained circular peptides in the CX_7C and $CX_{10}C$ formats, whereas the $CX_3CX_3CX_3C$ exhibits a more complicated and presumably variable disulfide bond pattern depending on the other residues. At the N terminus, all peptides carry the sequence MGSADGA. At the C terminus, a GAAG sequence links them to domain 1 (D1) of the phage coat protein g3p. The theoretical diversity of the combined libraries is $>10^9$. To provide a bait different from that used in other screenings of the same library for PAI-1 binding sequences (Dupont et al., 2006; Jensen et al., 2006), we used glycosylated PAI-1, which had been inactivated by bis-ANS, SDS, or XR5118, as a bait. PAI-1 was immobilized on the monoclonal anti-PAI-1 antibodies mAb-1 or mAb-5, respectively (Munch et al., 1991; Bødker et al., 2003), using alternating antibodies for different rounds of selection to avoid enrichment of antibody-binding phages. Six rounds of selection were performed. Of 64 phage clones investigated by ELISA, one demonstrated PAI-1-binding. Its sequence was CAASCLRECTFRCGADGACRRKCDMYCLKVC. This is a concatamer consisting of two sequences, each of the format $CX_3CX_3CX_3C$. Between them is the sequence GADGA, reminiscent of the sequence MGSADGA normally found at the N terminus of the peptides. This sequence, with a format not expected to be in the library, probably results from a cloning artifact during the construction of the library. The peptide will be referred to as paionin-4.

To be able to analyze binding of paionin-4 to PAI-1 by methods different from phage ELISA, we made a fusion protein consisting of the paionin-4 sequence fused to domain 1 and 2 of the phage coat protein g3p (Fig. 1). Domain 1 and 2 were chosen as the fusion partner, because they represent the natural scaffold for the peptides in the phages. A control protein, consisting of D1D2 without a peptide, was made as a control. Paionin-4-D1D2 as well as D1D2 migrated as sharp peaks in gel filtration and in reducing and nonreducing SDS-PAGE. In SDS-PAGE, there were only traces of more slowly migrating material, probably dimers (Fig. 1), indicative of homogeneous preparations largely free of multimers. An initial screening of binding of latent PAI-1 to paionin-4-D1D2 by FPLC gel filtration confirmed the binding, although we observed no binding of D1D2 without a peptide. In addition, paionin-4-D1D2, but not D1D2, was able to compete for paionin-4 phage binding in ELISA (data not shown). Thus, it seems that paionin-4-D1D2 exhibits the expected PAI-1 binding. To analyze the importance of separate parts of paionin-4, we decided also to make deletion mutants of the paionin-4 sequence. Each of the two four-cysteines motives and one overlapping sequence were constructed. Deletion of any part of the paionin-4 sequence resulted in nonbinding variants, as evaluated by FPLC assays and ability to compete phage binding (data not shown). Thus, the disulfide-bridged constrained fold of the entire peptide is crucial for the binding to PAI-1.

Functional Effects of Paionin-4 on PAI-1. We incubated PAI-1 in the absence or presence of paionin-4-D1D2 or,

as a control, D1D2 without peptide. After incubation for various time periods, aliquots were withdrawn for determination of the specific inhibitory activity. Without additions at 25 and 37°C, PAI-1 lost its activity with a half-life of approximately 700 and 65 min, respectively, as a result of conversion of PAI-1 to the inactive latent state. With 10 or 20 μM paionin-4-D1D2, the activity was lost at an approximately 2-fold faster rate. Paionin-4 also increased the rate of activity loss of the stable PAI-1 variant (14-1B, N152H-K156T-Q321L-M356I), which has a very slow latency transition rate (Berkenpas et al., 1995). In contrast, the effect on W177F, which also has a slow latency transition rate (Blouse et al., 2003), was small. There was no effect on the half-life of murine PAI-1. It is noteworthy that vitronectin abolished the effect of paionin-4-D1D2 on the rate of latency transition (Table 1).

We wished to confirm that the faster rate of activity loss in the presence of paionin-4-D1D2 was actually due to a faster rate of latency transition. With this aim, we used two independent assays for latency transition. First, we employed phage with the peptide sequence paionin-3, which we previously demonstrated can be used as a specific probe for latent PAI-1, because it binds to a site exposed upon extraction of β-strand 1C during latency transition (Dupont et al., 2006). We found that during incubations at 37°C, the binding affinity to paionin-3 phage increased with a rate indistinguish-

able from the rate by which activity was being lost. In four independent experiments, the half-life for the approach toward maximal paionin-3 phage binding was 56 ± 7 min without additions, 27 ± 3 min in the presence of 10 μM paionin-4-D1D2, and 49 ± 11 min in the presence of 10 μM D1D2 (Fig. 2), values matching the half-lives for activity loss listed in Table 1. Second, we took advantage of previous work demonstrating that the labeling of the P9 position of PAI-1 (S340C) with the environmentally sensitive fluorescent probe NBD produces a PAI-1 variant (PAI-1$_{P9-NBD}$) in which the RCL insertion occurring during latency transition may be followed by fluorescence spectroscopy (Shore et al., 1995). Full insertion of the P9-NBD-labeled RCL as s4A results in a sizable fluorescence increase that is consistent with transfer of the probe from a solvent exposed to a more hydrophobic environment. Figure 3 illustrates the fluorescence emission spectrum of the PAI-1$_{P9-NBD}$ variant before and after incubation with or without paionin-4-D1D2 for 7 days at 25°C. The spectrum after the extended incubation showed a severalfold enhancement in NBD fluorescence with the expected ~10-nm blue shift in peak emission from 543 to 533 nm, previously shown to accompany loop insertion during latency (Shore et al., 1995). The net fluorescence enhancement was significantly greater in the presence of paionin-4-D1D2 than in its absence. The fluorescence spectrum of PAI-1$_{P9-NBD}$ in the presence of paionin-4-D1D2 corresponded to that
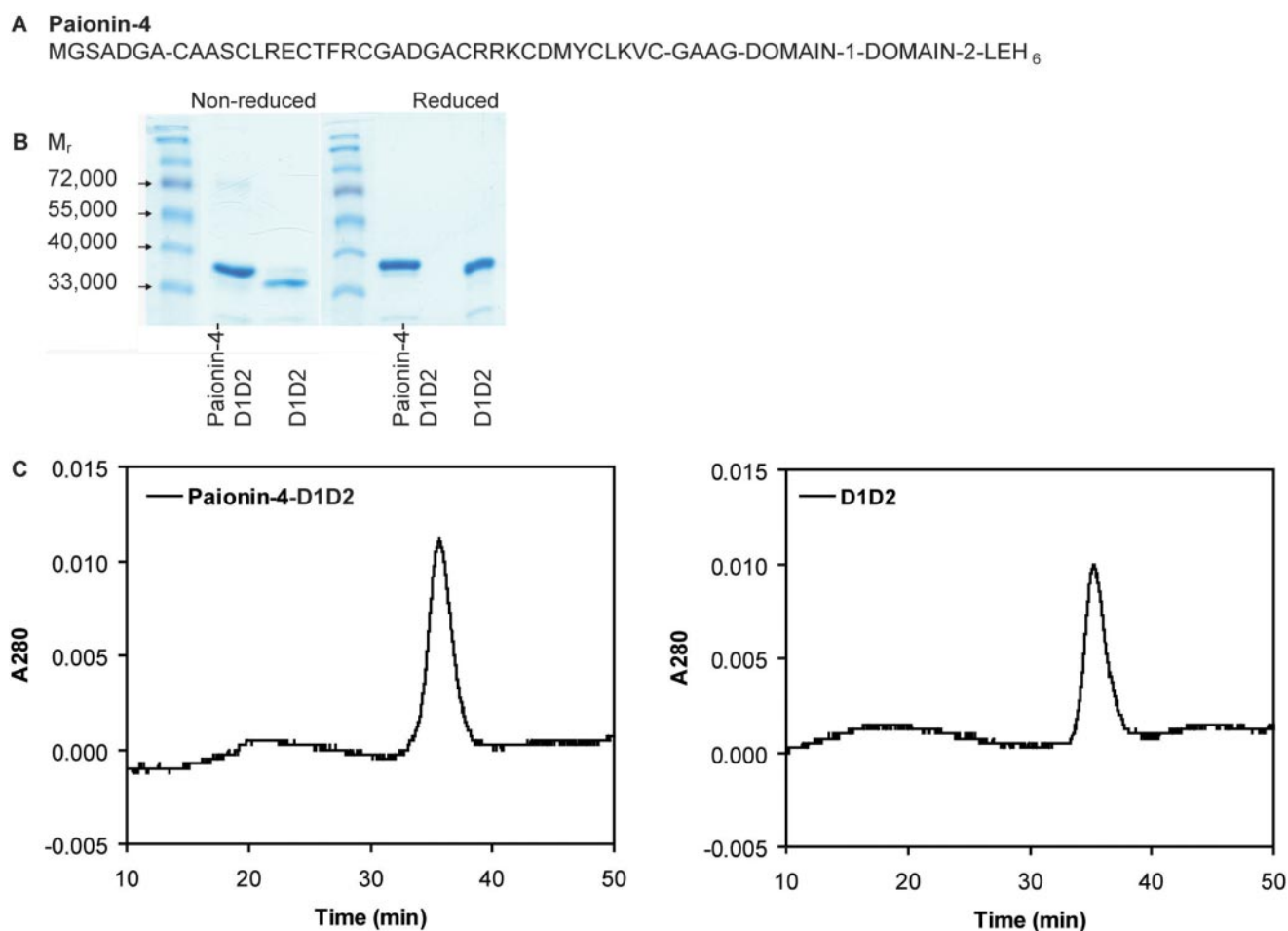
Fig. 1. Construction of paionin-4-D1D2 fusion protein. A, amino acid sequence of paionin-4-D1D2. B, SDS-PAGE of paionin-4-D1D2 and D1D2 under reducing and nonreducing conditions. The gels were stained with Coomassie Blue. C, Superose 12 gel filtration profiles of paionin-4-D1D2 and D1D2.

achieved by full loop insertion (data not shown). Incubation in the absence of paionin-4-D1D2 gave an amplitude of only approximately half of that, corresponding to a rate constant of approximately 2×10^{-4} min^{-1}. The fact that this is somewhat slower than expected from the data in Table 1 can be accounted for by the P9-NBD probe delaying loop insertion (Shore et al., 1995). From these two lines of evidence, we concluded that the faster rate of activity loss in the presence of paionin-4-D1D2 was due to an increased rate of latency transition.

Analysis of the Binding of Paionin-4 to Different Conformational Forms of PAI-1 by Surface Plasmon Resonance. To obtain a quantitative estimation of the binding of paionin-4 to PAI-1, we immobilized the paionin-4-D1D2 fusion protein on a BIACORE chip and injected different conformational forms of PAI-1 in varying concentrations. As a control, we immobilized D1D2 without a peptide fusion partner and corrected the binding to the paionin-4-D1D2 chip for the binding to the D1D2 chip. The binding to D1D2 was always less than 1 response unit. The association and the dissociation of PAI-1 to the paionin-4-D1D2 chip occurred very fast, preventing us from determining rate constants. This particular interaction was consequently analyzed under conditions yielding steady-state binding. An analysis of the concentration dependence of the steady-state binding showed that the data fitted well to a simple 1:1 binding model and allowed an easy calculation of the K_D values (Table 2). uPA-complexed PAI-1 had a higher affinity to paionin-4-D1D2 than the preparations of active and latent PAI-1. uPA alone did not bind above background. There was a marginal differ-

ence in affinity between the preparation of latent and the preparation of active PAI-1, whereas the active 14-1B variant of PAI-1 had a lower affinity than active wt PAI-1.

Mapping of the Binding Site for Paionin-4 by Antibody and Heparin Competition. To obtain a crude mapping of the binding site for paionin-4 on PAI-1, we estimated the binding of paionin-4 phage particles to PAI-1 bound to various monoclonal antibodies. The binding of paionin-4 phages to PAI-1 in the presence of a variety of monoclonal anti-PAI-1 antibodies was investigated by a phage particle ELISA (Fig. 4). In the presence of the monoclonal antibodies MA33B8 and mAb-7, the phage binding was not above background level, indicating that these antibodies competed for phage binding and that the paionin-4 binding site overlaps with the epitopes for these two antibodies. Paionin-4 and heparin competed for binding to PAI-1, as revealed by a phage ELISA (data not shown).

Mapping of the Binding Site for Paionin-4 by Site-Directed Mutagenesis. The epitope for MA33B8 was previously mapped to the loop connecting α-helix D and β-strand 2A, β-strand 3A, and the loop connecting β-strands 2B and 3B (Gorlatova et al., 2003; Naessens et al., 2003). Heparin has been reported to bind in a region spanning α-helix E and α-helix D, the important residues being Lys82 and Lys90 (Ehrlich et al., 1992). These findings and the above results suggested to us that the binding site for paionin-4 might also be in the α-helix D region of PAI-1. To determine the binding site for paionin-4 more precisely, we screened approximately 45 mutants with Ala substitutions for paionin-4 binding in phage particle ELISA, using PAI-1 in the latent form. The

TABLE 1
Effect of paionin-4-D1D2 on PAI-1 stability

The specific inhibitory activity of the indicated PAI-1 variants was measured after varying time periods of incubation at 25°C or 37°C at a PAI-1 concentration of 400 nM with the indicated fusion protein additions. The half-life for latency transition was calculated from semilogarithmic plots of the specific inhibitory activity versus time. Means $\pm$ S.D. of at least three independent determinations are indicated.

| PAI-1 variant	Temperature	Peptide	Half-Life
	°C		min
Human wt	37	None	65 $\pm$ 4
Human wt + vitronectin	37	None	118 $\pm$ 24[a]
Human wt	37	1 μM paionin-4-D1D2	64 $\pm$ 4
Human wt	37	5 μM paionin-4-D1D2	44 $\pm$ 3[b]
Human wt	37	10 μM paionin-4-D1D2	37 $\pm$ 2[b]
Human wt	37	20 μM paionin-4-D1D2	36 $\pm$ 2[b]
Human wt + vitronectin	37	10 μM paionin-4-D1D2	114 $\pm$ 25[a]
Human wt	37	10 μM D1D2	60 $\pm$ 6
Human wt	37	20 μM D1D2	65 $\pm$ 6
Human wt	25	None	698 $\pm$ 4
Human wt	25	1 μM paionin-4-D1D2	533 $\pm$ 1[b]
Human wt	25	5 μM paionin-4-D1D2	426 $\pm$ 6[b]
Human wt	25	10 μM paionin-4-D1D2	403 $\pm$ 4[b]
Human wt	25	10 μM D1D2	625 $\pm$ 35
Stable PAI-1, 14–1B	37	None	6656 $\pm$ 746
Stable PAI-1, 14–1B	37	1 μM paionin-4-D1D2	6452 $\pm$ 498
Stable PAI-1, 14–1B	37	5 μM paionin-4-D1D2	4636 $\pm$ 896[b]
Stable PAI-1, 14–1B	37	10 μM paionin-4-D1D2	2887 $\pm$ 346[b]
Stable PAI-1, 14–1B	37	10 μM D1D2	6765 $\pm$ 1683
W177F	37	None	493 $\pm$ 68
W177F	37	1 μM paionin-4-D1D2	478 $\pm$ 40
W177F	37	5 μM paionin-4-D1D2	424 $\pm$ 18
W177F	37	10 μM paionin-4-D1D2	397 $\pm$ 19[b]
W177F	37	10 μM D1D2	470 $\pm$ 12
Murine wt	37	None	96 $\pm$ 9
Murine wt	37	1 μM paionin-4-D1D2	94 $\pm$ 8
Murine wt	37	5 μM paionin-4-D1D2	89 $\pm$ 11
Murine wt	37	10 μM paionin-4-D1D2	90 $\pm$ 9

[a] Significantly different from the half-life in the corresponding value in the absence of vitronectin ($P < 0.01$).
[b] Significantly different from the half-life in the absence of paionin-4-D1D2 fusion protein and/or from the half-life in the presence of the same concentration of D1D2 ($P < 0.01$).

mutants that had an unambiguously reduced binding to paionin-4 phage of more than 2-fold in phage ELISA were then characterized with respect to steady state binding to a paionin-4-D1D2-coated BIACORE chip at 1 μM PAI-1, a concentration slightly above K_D. The lack of saturation at this concentration ensures the possibility of detecting reduced binding caused by the mutations. The following mutants had a significantly reduced binding in both phage ELISA and BIACORE: Y81A, P87A, W88A, K90A, D91A, and E92A (Table 3). The mutated residues were therefore considered part of the paionin-4 binding site. Murine PAI-1 and two chimeras between murine and human PAI-1 also had reduced binding to paionin-4 (Table 3). The two chimeras were composed of
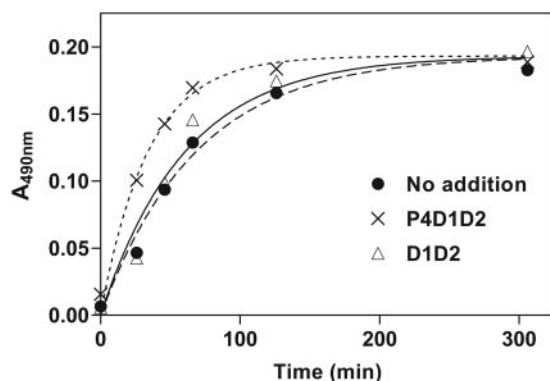
Fig. 2. Paionin-4 accelerates latency transition, as analyzed by paionin-3-phage ELISA. PAI-1 (110 nM), expressed from *E. coli*, was incubated at 37°C alone (●) or in the presence of 10 μM paionin-4-D1D2 (P4-D1D2) fusion protein (×) or 10 μM D1D2 (△). At different time points, samples were added to and incubated in the wells of a Microtiter plate coated with mAb-6, for 30 min at 25°C. The amount of latent PAI-1 captured on the solid phase was subsequently detected using paionin-3 phage. The signals from wells without PAI-1 were subtracted. The experimental data points were fit to a mono-exponential approach to steady-state (—, - - -, and — — —, respectively). The figure shows the result of one of four independent experiments. In the four experiments, the half-lives were 57 ± 11 (no additions), 27 ± 3 (with paionin-4-D1D2), and 49 ± 11 (with D1D2), corresponding to a statistically significant effect of paionin-4-D1D2 (*p* < 0.01), but not of D1D2.
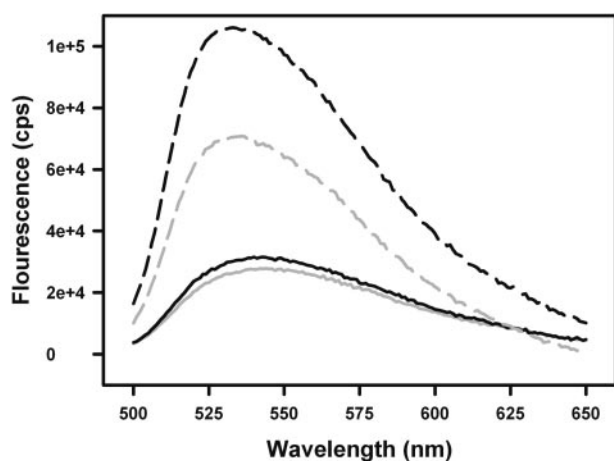
Fig. 3. Paionin-4 accelerates latency transition, as analyzed PAI-1$_{P9-NBD}$. Fluorescence emission spectra of PAI-1$_{P9-NBD}$ (50 nM) were recorded in the presence and absence of 500 nM paionin-4-D1D2 and incubation at 25°C for 7 days. PAI-1$_{P9-NBD}$ at *t* = 0 (gray —); PAI-1$_{P9-NBD}$ + paionin-4-D1D2 at t = 0 (—); PAI-1$_{P9-NBD}$ at t = 7 days (gray — — —); PAI-1$_{P9-NBD}$ + paionin-4-D1D2 at t = 7 days (— — —). All fluorescence spectra were acquired with an excitation wavelength at 480 nm and represent the averaged spectra of three independent experimental acquisitions.

the human and murine parts of PAI-1 N- and C-terminal to a conserved stretch of residues in hF.

Functional Effects of mAb-7. Based on the paionin-4-D1D2 phage ELISA, mAb-7 seems to have an epitope close to that of MA33B8 and to the binding site for paionin-4. We demonstrated previously that like MA33B8 (Verhamme et al., 1999), mAb-7 induces a rapid irreversible loss of inhibitory activity of PAI-1 (Gils et al., 2003). We therefore hypothesized that mAb-7, like MA-33B8, rapidly induces conversion to the latent state. To compare the mechanism for latency transition of paionin-4 to that for a latency-inducing antibody, we characterized the functional effect of mAb-7 on PAI-1 and its binding epitope on PAI-1 in detail. To provide evidence for latency-induction by mAb-7, we used two independent assays. We first employed the paionin-3 peptide phage ELISA as described above. Clearly, both mAb-7 and MA-33B8 induced paionin-3 phage binding, whereas a control anti-PAI-1 antibody had no effect on the binding (Fig. 5). Moreover, when mAb-7 was incubated with PAI-1$_{P9-NBD}$, we observed a rapid enhancement in the fluorescence emission and in the same manner as paionin-4, a ~10-nm blue shift in

TABLE 2
Analysis of the binding of different conformational forms of PAI-1 to paionin-4 by surface plasmon resonance

The steady-state binding of the indicated PAI-1 forms, in concentrations between 0.03 and 2 μM, to paionin-4-D1D2 was determined by the use of a BIACORE T100 instrument, with paionin-4-D1D2 immobilized on a CM5 chip. The K_D values were determined by plotting the steady-state binding of the different PAI-1 forms to the chips versus the injected concentrations of the various PAI-1 forms and fitting the data to the equation [PAI-1 bound] = ([paionin-4-D1D2] × [PAI-1])/(K_D + [PAI-1]). Means ± S.D. of three independent experiments are indicated.

PAI-1 Form	K_D
	nM
Active PAI-1	448 ± 54
Latent PAI-1	339 ± 15[a]
uPA-PAI-1 complex	195 ± 33[a]
PAI-1 14-1B	1020 ± 50[a]

[a] Significantly different from the value for active PAI-1 wt (*P* < 0.01).
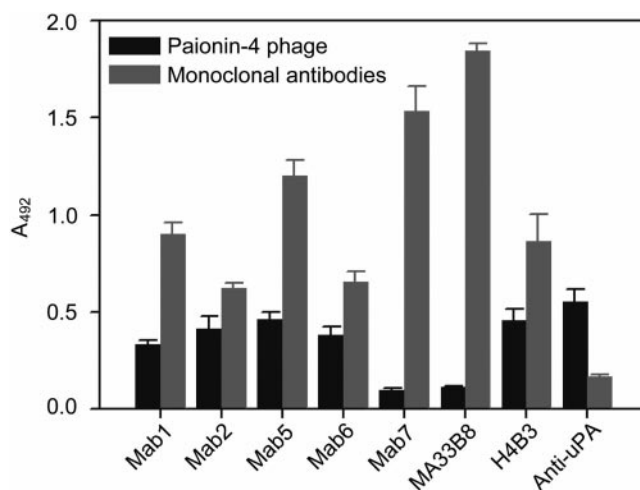
Fig. 4. Mapping of the binding site for paionin-4 by the use of monoclonal antibodies. Microtiter plates were coated with the polyclonal anti-PAI-1 antibody, pAb-4898. The next layer contained 0.5 μg/ml latent PAI-1. Paionin-4 phage and monoclonal antibodies were added simultaneously and allowed to react for 1 h. The amount of bound phage (black bars) or the amount of bound monoclonal antibody (gray bars) was estimated by a layer of HRP-conjugated anti-M13 antibody or a layer of HRP-conjugated rabbit anti-mouse antiserum, respectively. The figure displays mean and standard deviations for triple determinations in a typical experiment of a total of 3.

the emission peak that is characteristic for RCL insertion and transition to the latent conformation (Fig. 6A). A time course of antibody-induced latency by mAb-7 is shown in Fig. 6B for 25 nM PAI-1$_{P9-NBD}$ and 1.0 μN mAb-7. As was found for mAb MA33B8, the first-order rate constant increased linearly up to the highest concentration of mAb-7 tested (3.3 μN). The concentration dependence of the reaction on mAb-7 (Fig. 6B, inset) gave a calculated second-order rate constant of 1.78×10^4 M^{-1} s^{-1}, a rate very close to that reported for

TABLE 3
Alanine scanning analysis of PAI-1 residues involved in binding of paionin-4

Initially, 45 PAI-1 mutants in the latent state were tested for paionin-4 binding by the use of phage ELISA. The level of phage binding was expressed relative to that of the wt. The following mutants did not differ measurably (i.e., less than 2-fold) from wt with respect to binding to paionin-4 in phage ELISA: K82E, M85A, E92A, S94A, T96A, F100A, Q102A, P113A, F116A, F119A, R120A, S121A, T122A, K124A, Q125A, V126A, K143A, T144A, H145A, T146A, K147A, Y172A, Y174A, W177F, K178A, E214A, Y222A, D224A, H231A, D233A, Y243A, E244A, K245A, K325A, N331A, S333A. The mutants that demonstrated decreased binding in phage ELISA were then characterized further by the use of surface plasmon resonance, using a BIA-CORE T100 instrument equipped with paionin-4-D1D2, and, as a control for nonspecific binding, D1D2. The mutants were passed over the chip in concentrations of 1 μM. The levels of steady state binding were expressed relative to that of the wt. The table shows means and S.D. for at least three independent determinations. Also shown is the binding of PAI-1 wt to a chip with D1D2 (i.e., without paionin-4).

PAI-1 variant	Secondary Structural Element	Binding in Phage ELISA	Binding in BIACORE
		fraction of control	
wt		1.00	1.00
Y81A	hD	0.14 ± 0.05^a	0.25 ± 0.03^a
P87A	hD-s2Aloop	0.23 ± 0.01^a	0.11 ± 0.01^a
W88A	hD-s2Aloop	0.18 ± 0.07^a	0.01 ± 0.02^a
K90A	s2A	0.36 ± 0.06^a	0.27 ± 0.00^a
D91A	s2A	0.17 ± 0.06^a	0.11 ± 0.01^a
E92A	s2A	0.17 ± 0.06^a	0.40 ± 0.14^a
Murine wt		N.D.	0.15 ± 0.01^a
Murine-hF-human chimera		N.D.	0.39 ± 0.06^a
Human-hF-murine chimera		N.D.	0.06 ± 0.00^a
wt, D1D2 chip			-0.01 ± 0.04^a

N.D., not determined, because the murine and murine-human chimeras react differently from the human protein with the antibodies employed in the ELISA.
^{a} Significantly different from wt binding to the paionin-4-D1D2 according to Student's t-test ($P < 0.01$).

Fig. 5. mAb-7 induces PAI-1 latency transition, as analyzed by paionin-3-phage ELISA. PAI-1 (10 nM), expressed from *E. coli*, in the presence of mAb-5, mAb-7 or MA33B8, was added to and incubated in the wells of a Microtiter plate coated with mAb-6, for 30 min at 25°C. The amount of latent PAI-1 captured on the solid phase was subsequently detected using paionin-3 phage (white bars). To verify that equal amounts of PAI-1 had been captured on the solid phase in the presence of each of the three antibodies, a parallel ELISA was performed in which PAI-1 was detected using polyclonal rabbit anti-PAI-1 antibody pAb-4898 (black bars). The bars represent the mean and S.D. for three independent experiments. The signal from wells without PAI-1 have been subtracted.

MA33B8 (Verhamme et al., 1999). On the basis of these findings, we concluded that mAb-7 indeed causes a rapid conversion to the latent state in a manner analogous to MA33B8.

Next, we compared the binding of wt PAI-1 in active, latent, and uPA-complexed state to mAb-7 by the use of surface plasmon resonance, with mAb-7 coupled to a CM5 chip (Fig. 7). Active PAI-1 wt bound at most slightly more slowly to a mAb-7-coated chip than latent PAI-1 wt and uPA wt PAI-1 complex. When passing uPA over a mAb-7 chip saturated with active wt PAI-1, there was no measurable binding. The binding of latent PAI-1 W177F occurred at a rate indistinguishable from that of latent PAI-1 wt, but the binding of active PAI-1 W177F occurred approximately 5-fold more slowly than binding of active wt PAI-1; W177F has a considerably slower latency transition rate than wt PAI-1 (Table 1). But again, uPA was unable to bind to the mAb-7–

Fig. 6. mAb-7 induces PAI-1 latency transition, as analyzed by PAI-1$_{P9-NBD}$. A, fluorescence emission spectra of PAI-1$_{P9-NBD}$ (50 nM) were recorded before (—) and after (— — —) incubation for 20 min at 25°C with mAb-7 or an antibody of irrelevant specificity, anti-uPA mAb-12 (gray — and — — —, respectively). The antibodies were present in a final concentration of 500 nM. All fluorescence spectra were acquired with an excitation wavelength at 480 nm and represent the averaged spectra of three experimental acquisitions. B, time course of the mAb-7 (1.0 μN) induced enhancement in NBD fluorescence of 25 nM PAI-1$_{P9-NBD}$. The dependence of k_{obs} on mAb-7 concentration (inset). The slope of the best fit regression line has an intercept near zero and corresponds to a second-order rate constant of 1.78×10^4 M^{-1} s^{-1}.

coated chip saturated with PAI-1 W177F. Moreover, when the stable PAI-1 variant 14-1B, with an extremely slow latency transition, was passed over the chip in its active state, there was no measurable binding even at 250 nM (Table 5). These results are consistent with the notion that with the time resolution possible with the BIACORE, active PAI-1 is converted to latent PAI-1 as it binds to mAb-7 on the chip.

Mapping the Epitope for Anti-PAI-1 mAb-7. We next mapped the epitope for mAb-7 by the use of site-directed mutagenesis. We first measured the IC_{50} values for the inactivation of wt and mutant PAI-1 by this antibody (Table 4). The IC_{50} value for inactivation of PAI-1 by mAb-7 was found to increase more than 2-fold with the substitutions P87A, W88A, K90A, D91A, W177F, K178A, and H231A. The stable variant of PAI-1, 14-1B, also had a strongly increased IC_{50} value. Murine PAI-1 and the two murine-human PAI-1 chimeras showed strongly increased IC_{50} values as well. A number of residues were by the same strategy excluded from the epitope.

We next studied the binding of the substitution mutants by surface plasmon resonance. Because active PAI-1 seems to be converted to the latent form when binding to mAb-7 immobilized on a BIACORE chip (see *Functional Effects of mAb-7*), the K_D values for PAI-1 binding to mAb-7 could only be determined meaningfully with latent or uPA-complexed PAI-1, and we decided to test the effect of the substitution mutations by the use of latent PAI-1. For each mutant, we determined the association rate constant, the dissociation rate constant, and the K_D as the ratio between the rate constants (Table 5). The affinities for binding of latent and uPA-complexed PAI-1 to mAb-7 were high with K_D values being around 50 pM. The mutants W88A, K90A, D91A, K178A, and H231A had significantly increased K_D values. It is noteworthy that the mutants P87A and W177F did not differ from wt with respect to K_D, although their IC_{50} values did (Table 4). In addition, the stable PAI-1 variant, being used in the active state, showed no measurable binding, and murine PAI-1 and the two murine-human chimeras had a strongly reduced binding. The variation in the K_D values was due mainly to variation in the dissociation rate constant. On the basis of these findings, we concluded that mAb-7 has an epitope overlapping with the binding site for paionin-4, in agreement with the fact that the two compete for binding.

Discussion

In this report, we describe studies aimed at isolating novel types of inactivators of PAI-1, a therapeutic target in cancer and cardiovascular diseases. A variety of low molecular mass organochemicals have been found to inhibit PAI-1's antiproteolytic activity (for review, see Andreasen, 2007). PAI-1-inactivating diketopiperazine derivatives (Bryans et al., 1996; Charlton et al., 1996; Charlton et al., 1997; Friederich et al., 1997; Folkes et al., 2001; Wang et al., 2002; De Nanteuil et al., 2003) were by a variety of biochemical analyses shown to induce a stable, inactive PAI-1 conformation, which is different from other known PAI-1 conformations (Einholm et al., 2003). A number of negatively charged, amphipathic organochemical compounds of diverse chemical structures were reported to inactivate the antiproteolytic effects of PAI-1 (Urano et al., 1992; Munch et al., 1993; Björquist et al., 1998; Egelund et al., 2001a; Gils et al., 2002; Crandall et al., 2004). Available evidence, based on competition with monoclonal antibodies with known epitopes, site-directed mutagenesis, and molecular modeling, suggests that these compounds bind in a hydrophobic pocket beneath α-helix D (Björquist et al., 1998; Egelund et al., 2001a; Gorlatova et al., 2007). They rapidly induce PAI-1 substrate behavior, followed by polymerization (Egelund et al., 2001a; Pedersen et al., 2003). In addition, many monoclonal antibodies have been found to inactivate PAI-1, either by steric hindrance of the binding of the protease, by inducing substrate behavior, or by rapidly converting PAI-1 to the latent state (for review, see Gils and Declerck, 2004).

We have chosen to explore the possibilities of deriving PAI-1-inactivating peptides from phage-displayed libraries. Our previous experience with such peptides suggests that they, in contrast to organochemical compounds, are likely to have specificities comparable with those of monoclonal antibodies, for instance having very different affinities to different conformations (Hansen et al., 2005; Sumbayev et al., 2005; Dupont et al., 2006; Andersen et al., 2008). In contrast to organochemicals, they do not bind to serum albumin. In contrast to monoclonal antibodies, their small size allows for chemical modifications, for instance by insertion of non-natural amino acids. The first peptide designed to inhibit a serpin had a sequence corresponding to that of the part of the
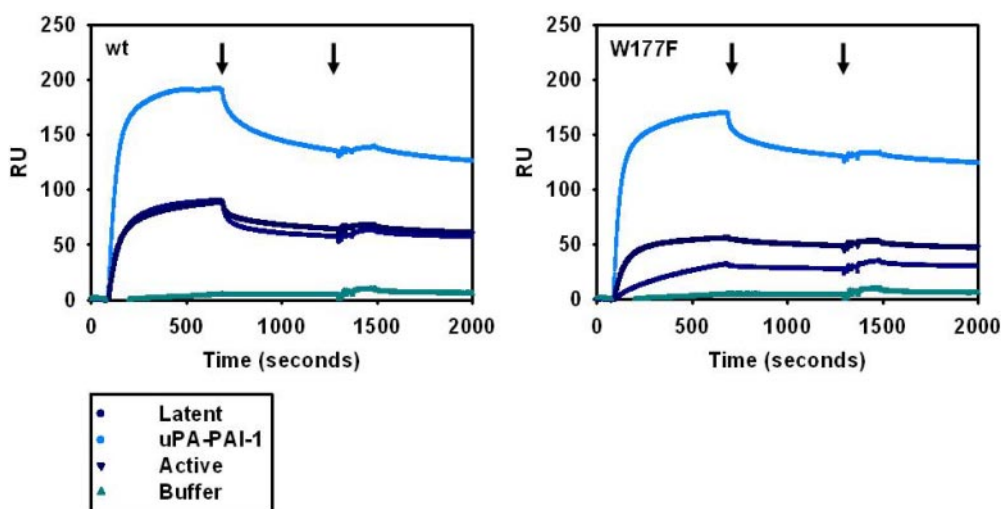
Fig. 7. mAb-7 converts active PAI-1 to the latent form as it binds. mAb-7 (200 response units) was immobilized on a BIACORE chip. From 100 to 500 s, wt or latent PAI-1 W177F (8 nM), wt or active PAI-1 W177F (8 nM), wt or active PAI-1 W177F (8 nM) plus uPA (16 nM), or buffer was passed over the chip at a flow rate of 30 μl/min. After an additional 600 s, uPA (16 nM) was in all cases passed over the chip (arrow). The color symbols were as indicated in the figure. The small rapid decline in binding after stop of the first injection (arrow) is due to the surface plasmon resonance phenomenon referred to as "bulk" effect.

RCL that normally inserts in β-sheet A upon complex formation; such peptides occupy the place of the RCL in the sheet and induce substrate behavior (Schulze et al., 1990). From a phage-displayed peptide library, we previously isolated a peptide inhibiting the binding of protease-PAI-1 complexes to endocytosis receptors (Jensen et al., 2006). In the present report, we describe the isolation of a peptide sequence, paionin-4, which accelerates the rate of conversion of PAI-1 to the latent state.

The possibility of inactivating PAI-1 by converting it to the latent state was originally suggested on the basis of investigations of inactivation of PAI-1 by the monoclonal anti-PAI-1 antibody MA33B8 (Verhamme et al., 1999). MA33B8 binds

TABLE 4

Mapping of the epitope for mAb-7 by site-directed mutagenesis and IC_{50} determinations

To determine the IC_{50} values, PAI-1 was serially diluted at 37°C to concentrations between 0.4 and 400 nM and incubated for 20 min in the presence of mAb-7 in concentrations ranging from 0 to 80 nM. uPA was then added in portions of 25 μl to a final concentration of 10 nM. After 5 min, the remaining uPA activity was determined and the specific inhibitory activity of PAI-1 determined from the PAI-1 concentration giving half-inhibition of the added uPA. The IC_{50} values for the antibodies were determined from plots of the specific inhibitory activity of PAI-1 against the antibody concentration in the final assay mixture, because the antibody concentration reducing the specific inhibitory activity to 50%. Mean, S.D., and number of determinations are indicated. The following mutants had an IC_{50} value less than 2-fold higher than that of wt: Y81A, H85A, E92A, S94A, T96A, K143A, T144A, H145A, T146A, K147A, Y172A, N174A, K176A, D233A, K325A, N331A, S333A.

PAI-1 variant	Secondary Structural Element	IC_{50}
		nM
Human wt		23.0 ± 6.0 (4)
Human P87A	hD-s2A loop	62.6 ± 12.4 (3)[a]
Human W88A	hD-s2A loop	>100 (3)[a]
Human K90A	s2A	>100 (5)[a]
Human D91A	s2A	95.0 ± 10.0 (3)[a]
Human W177F	s3A	67.2 ± 20.4 (4)[a]
Human K178A	s3A	63.8 ± 24.9 (6)[a]
Human H231A	s2B-s3B loop	95.0 ± 10.0 (3)
Human 14–1B	hF-s3A loop, s5A, s1C	86.2 ± 12.3 (3)[a]
Murine wt		90.0 ± 14.1 (2)[a]
Murine-hF-human chimera		87.1 ± 14.9 (2)[a]
Human-hF-murine chimera		>100 (2)

[a] Significantly different from wt according to Student's *t* test ($P < 0.01$)

preferentially to RCL-inserted forms of PAI-1. The theory originally proposed for the mechanism of action of MA33B8 was therefore that exposure of its epitope was coupled to at least a partial insertion of the RCL into β-sheet A. Because the conversion to the latent state is virtually irreversible, the observed antibody effect cannot be explained as a shifting of the equilibrium between active and latent forms toward the latent form. Therefore, the concept of a "prelatent" state was formulated. The prelatent state would be in equilibrium with the active state and would be more rapidly converted to the latent state than active PAI-1. Exposure of the MA33B8 epitope in the prelatent state would allow the antibody to stabilize this conformation, thereby shifting the equilibrium in favor of the prelatent state and consequently accelerating latency transition (Verhamme et al., 1999). By mapping the epitope of another antibody, H4B3, we recently provided evidence that the prelatent state involves the extraction of β-strand 1C from the β-sheet A, presumably coupled to the partial insertion of the RCL into β-sheet A (Dupont et al., 2006). In the present report, we have substantiated the concept of the prelatent state. We show that another antibody, mAb-7, which also inactivates PAI-1, has an epitope overlapping with that of MA33B8, and, by the use of a peptidyl probe for latent PAI-1, surface plasmon resonance binding analysis, and fluorescence spectroscopy, demonstrate that binding of PAI-1 to the antibody is indeed associated with a fast conversion to the latent state.

Most importantly, we here report that the strategy of accelerating latency transition is also feasible with a molecule much smaller than an antibody. Paionin-4 has a binding site overlapping with those of MA33B8 and mAb-7. The conclusion, that paionin-4 induces the latent state and not another inactive form was based on the use of a peptidylic probe specific for latent PAI-1 and the fluorescent PAI-1 derivative $PAI-1_{P9-NBD}$. However, there are several important differences between the effect of paionin-4 and the effect of the antibodies. First, whereas the antibodies convert PAI-1 to the latent state within seconds, the peptide merely causes an up to 3-fold acceleration of the rate of latency transition. Second, the K_D values for binding of mAb-7 to latent PAI-1 was here observed to be around 50 pM, whereas that of the peptide was

TABLE 5

Mapping of the epitope for mAb-7 by site-directed mutagenesis and surface plasmon resonance

The binding of PAI-1 wt and mutants to mAb-7 was analyzed by surface plasmon resonance with a BIACORE T100 instrument, by injecting the PAI-1 variants, in the latent or uPA-complexed form, in concentrations between 0.25 and 500 nM over a BIACORE CM5 chip coated with 200 response units of mAb-7. The association (k_1) and dissociation (k_{-1}) rate constants and the equilibrium dissociation constant (K_D) were determined by a global fit to the data according to a 1:1 binding model.

The following mutants showed no significant change in mAb-7 binding, as evaluated by BIACORE: Y81A, H85A, P87A, E92A, S94A, T96A, K143A, T144A, H145A, T146A, K147A, Y172A, N174A, W177F, D233, K325A, N331A, S333A.

PAI-1 variant	Secondary Structural Element	k_1	k_{-1}	K_D
		$\mu M^{-1} s^{-1}$	$s^{-1} \times 10^4$	*nM*
Human wt		4.25 ± 2.26 (5)	1.93 ± 0.95 (5)	0.0517 ± 0.0263 (5)
Human wt in complex with uPA		7.96 ± 0.89 (3)	2.12 ± 0.84 (3)	0.0365 ± 0.0240 (3)
Human W88A	hD-s2A loop	2.62 ± 0.76 (2)	30.8 ± 6.6 (2)[a]	1.19 ± 0.09 (2)[a]
Human K90A	s2A	0.100 ± 0.058 (2)	15.3 ± 3.0 (2)[a]	17.5 ± 7.2 (2)[a]
Human D91A	s2A	0.619 ± 0.213 (2)	14.8 ± 1.3 (2)[a]	2.58 ± 1.11 (2)[a]
Human K178A	s3A	2.64 ± 0.04 (2)	6.12 ± 2.30 (2)[a]	0.233 ± 0.090 (2)[a]
Human H231A	s2B-s3B loop	2.27 ± 0.61 (2)	78.9 ± 3.8 (2)[a]	3.63 ± 1.14 (2)[a]
Human 14–1B[b]	hF-s3A loop, s5A, s1C	No binding measurable at 250 nM[b]		
Murine wt		No binding measurable at 250 nM		
Murine-hF-human chimera		4.67 ± 1.00 (2)	36.7 ± 4.4 (2)[a]	0.794 ± 0.076 (2)[a]
Human-hF-murine chimera		0.165 ± 0.244 (3)	182 ± 12 (3)[a]	330 ± 222 (3)[a]

[a] Significantly different from the corresponding value for wt ($P < 0.01$).
[b] In contrast to the other mutants, this one was applied to the BIACORE in the active form, because it is not possible to prepare a purely latent preparation of it as a result of the slow latency transition rate.

around 300 nM. Third, the antibodies do not bind measurably to active PAI-1: by surface plasmon resonance binding analysis, we provided evidence that active PAI-1 is converted to the latent state during or very shortly after binding to mAb-7. In contrast, the difference in affinity of the peptide to the latent and active states was less than 10-fold. Fourth, although overlapping, the binding site for the peptide and the epitopes for the antibodies differed in important respects. Our data here are consistent with the idea that Trp88, Lys90, Asp91, Lys178, His231 are part of the epitope for mAb-7.

Thus, the epitope includes residues on three different secondary structural elements. In contrast, the residues mapped to the paionin-4 binding site were all, except Tyr81, localized to a single secondary structural element. This fact may underlie the much smaller difference in affinity between active and latent forms of PAI-1 for paionin-4 than for the antibodies. Nevertheless, the position of the residues in the paionin-4 binding site does vary between the three-dimensional structures of active and latent PAI-1 (Fig. 8). In addition, it is remarkable that paionin-4 had a strongly reduced binding to
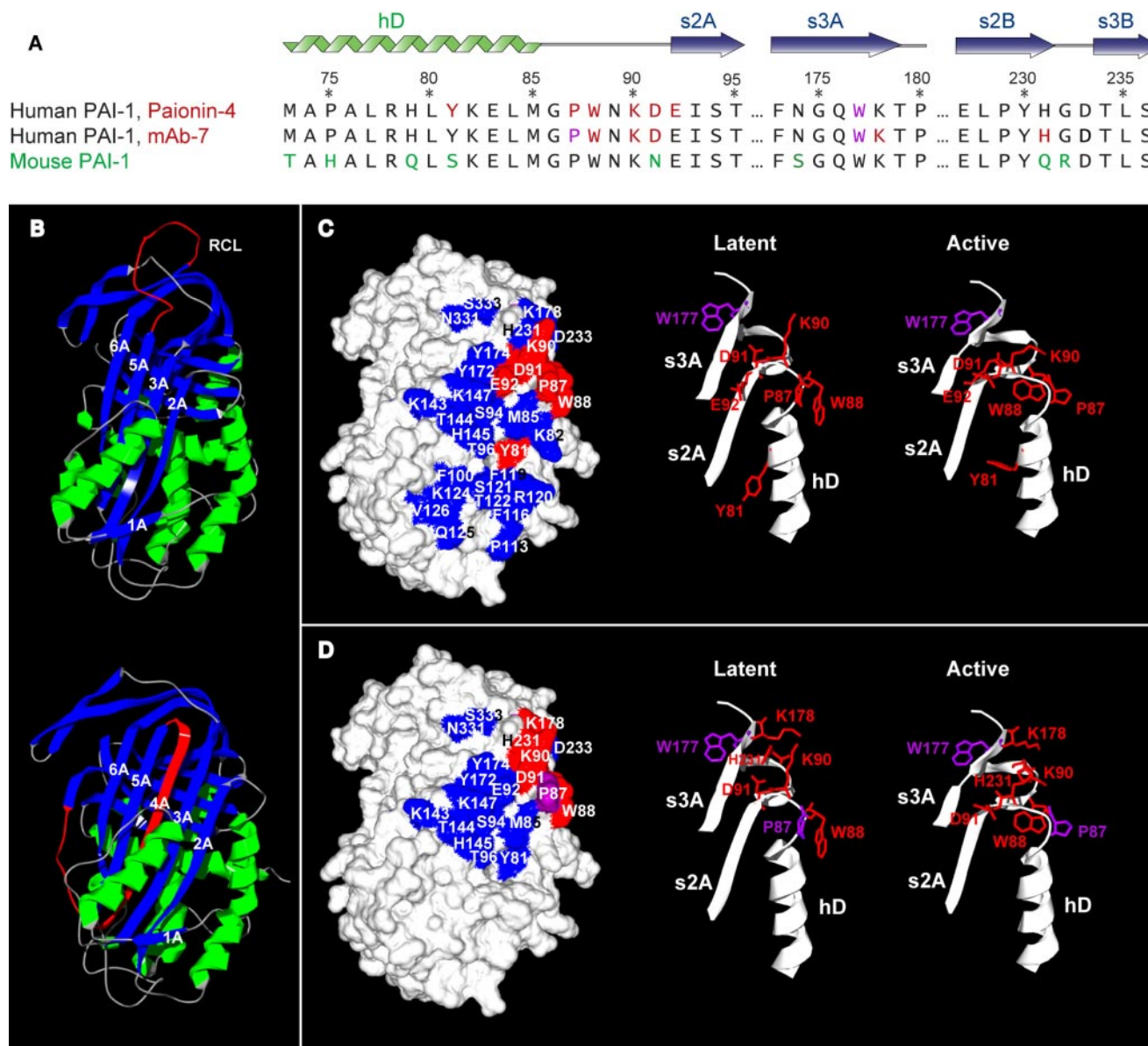
Fig. 8. The binding sites of paionin-4 and mAb-7 in PAI-1. A, amino acid sequence of the regions in PAI-1 containing the binding sites for paionin-4 and mAb-7 and comparison to the sequence of mouse PAI-1. The residues implicated in binding to paionin-4 or mAb-7 are shown in red. Residues that were found to have a decreased latency transition rate but not were implicated in the binding site are shown in purple. The residues in mouse PAI-1 that are different from those in human PAI-1 are shown in green. B, the three-dimensional structure of PAI-1. Ribbon representations of the structures of active PAI-1 (top panel) and latent PAI-1 (left panel). The reactive center loop (RCL) is shown in red, β-sheets in blue and α-helices in green. C, residues implicated in the binding site for paionin-4 are shown in red and those that were shown not to be implicated are shown in blue, displayed on a surface presentation of latent PAI-1 (left), and a ribbon presentation of the α-helix D-β-strand 2A area of latent PAI-1 (middle) and of active PAI-1 (right) with the residues implicated in the binding site shown in red. D, residues implicated in the epitope for mAb-7, displayed on a surface presentation of latent PAI-1 (left), a ribbon presentation of the α-helix D-β-strand 2A area of latent PAI-1 (middle), and of active PAI-1 (right) with the residues implicated in the binding site shown in red. Shown in purple are Pro87 and Trp177, which are not part of the binding site but affect the functional response of PAI-1 to paionin-4. All figures were constructed with Swiss-PDB-Viewer 3.7 and Pov-Ray 3.5 on the basis of the coordinates given in PDB entries 1DVM and 1DVN (Stout et al., 2000).

both the human-hF-murine PAI-1 chimera and the murine-hF-human chimera. If paionin-4 binding had depended only on residues in α-helix D and the α-helix D-β-strand 2A loop, the human-hF-murine chimera should have bound paionin-4 as well as human PAI-1. It therefore seems that the conformation of the paioin-4 binding site also depends on residues in other secondary structural elements and that the effect of paionin-4 may indeed depend on the conformational changes of PAI-1. Fifth, mAb-7 and paionin-4 differed with respect to their response to vitronectin: although the effect of mAb-7 is independent of the absence or presence of vitronectin (Gils et al., 2003), we showed here that vitronectin protects PAI-1 against paionin-4. Vitronectin has a very low affinity to latent PAI-1 (for review, see Wind et al., 2002). In this respect, paionin-4 resembles all the organochemical PAI-1 inactivators isolated to date (for a review, see (Andreasen, 2007). However, it is not known how fast PAI-1, after having been secreted from cells, reacts with vitronectin relative to its reaction with plasminogen activators. Indeed, the compound PAI-039 from which vitronectin protects PAI-1 in vitro, works well in vivo (Gorlatova et al., 2007). Sixth, the observations concerning the differential reaction of stable PAI-1 14-1B and PAI-1 W177F to mAb-7 and paionin-4 are remarkable. Whereas the stable PAI-1 variant 14-1B and PAI-1 W177F were both resistant to mAb-7, 14-1B seemed to react readily to paionin-4, whereas PAI-1 W177F had a somewhat reduced susceptibility. In the latent state, PAI-1 W177F mutant and wt PAI-1 demonstrated indistinguishable binding to both compounds, showing that Trp177 is not part of their binding sites. It is also clear that the residues mutated in 14-1B are distant from the binding for mAb-7 or paionin-4. But on the basis of the concept of the prelatent state, the decreased susceptibility of these mutants to mAb-7 is readily explained by the assumption that the prelatent state is less populated in the mutants than in wt. This notion is in agreement with the fact that both mutants have a reduced latency transition rate also in the absence of mAb-7. Thus, given the high susceptibility of 14-1B to paionin-4, comparable with that of wt, one would have to conclude that paionin-4 induces latency by a mechanism different from that of mAb-7. Taken together, all these differences suggest that in spite over the overlapping binding sites, the antibodies and paionin-4 accelerate latency transition by different mechanisms, the concept of the prelatent state being unable to explain the effect of paionin-4. Instead, we would like to suggest that paionin-4 induces a change facilitating loop insertion and acts by stabilizing the transition state between active and latent PAI-1.

Despite these differences, both paionin-4-D1D2 and mAb-7 bind as well to the uPA-PAI-1 complex as to latent PAI-1. This observation suggests a similar conformation of their common binding area in the two RCL-inserted forms.

Because our results here demonstrate that acceleration of latency transition can be achieved with a relatively small molecule, we believe our results represent an important step forward in providing strategies that may be employed for pharmacological inactivation of PAI-1. In the present case, paionin-4 has 31 residues and an effect likely to depend on a fold stabilized by a complicated disulfide bridge pattern, so the molecular recognition between the peptide and PAI-1 may indeed resemble that of an antibody. An important next step will be determination of the disulfide-bridge pattern of paionin-4. At the present stage, we have only used paionin-4

as a fusion protein with the 2 N-terminal domains of the phage coat protein g3p, D1 and D2. It is therefore important to state that there is no reason to believe that the paionin-4 peptide sequence does not fold as an independent domain in the fusion protein and that the effects observed are not those of the paionin-4 peptide sequence as such. Peptides displayed by the library employed here cannot fold in a way implying a common disulfide bridge pattern with the domains of the phage coat protein, because intact phage coat proteins are needed to form mature, infectious phage particles. The phages used here, with their peptide insertions, are indeed infectious, because no helper phages are needed. Moreover, the peptides fold the same whether they are displayed on the phages or are expressed recombinantly in fusion with D1D2, as paionin-4-D1D2 fusion protein and paionin-4 phages compete for binding to their target (see *Results*). It therefore follows that also paionin-4, both when inserted in the phage and when fused to D1D2, has the disulfide bridge pattern determined by its sequence and giving the highest stability. We would also like to draw the attention to the fact that the fusion proteins migrate as sharp peaks in gel filtration and nonreducing SDS-PAGE (Fig. 1). If folding had been abnormal and heterogeneous, formation of oligomers would have been expected. An important next step will be to affinity-mature this peptide to achieve a higher affinity to PAI-1 and mapping of the PAI-1 binding area of paionin-4 by site-directed mutagenesis.

References

Andersen LM, Wind T, Hansen HD, and Andreasen PA (2008) A cyclic peptidylic inhibitor of murine urokinase-type plasminogen activator: Changing species specificity by substitution of a single residue. *Biochem J* **412:**447–457.

Andreasen PA (2007) PAI-1 - a potential therapeutic target in cancer. *Curr Drug Targets* **8:**1030–1041.

Andreasen PA, Egelund R, Jensen S, and Rodenburg KW (1999) Solvent effects on activity and conformation of plasminogen activator inhibitor-1. *Thromb Haemost* **81:**407–414.

Andreasen PA, Egelund R, and Petersen HH (2000) The plasminogen activation system in tumor growth, invasion, and metastasis. *Cell Mol Life Sci* **57:**25–40.

Andreasen PA, Kjøller L, Christensen L, and Duffy MJ (1997) The urokinase-type plasminogen activator system in cancer metastasis: a review. *Int J Cancer* **72:**1–22.

Berkenpas MB, Lawrence DA, and Ginsburg D (1995) Molecular evolution of plasminogen activator inhibitor-1 functional stability. *EMBO J* **14:**2969–2977.

Björquist P, Ehnebom J, Inghardt T, Hansson L, Lindberg M, Linschoten M, Strömqvist M, and Deinum J (1998) Identification of the binding site for a low-molecular-weight inhibitor of plasminogen activator inhibitor type 1 by site-directed mutagenesis. *Biochemistry* **37:**1227–1234.

Blouse GE, Perron MJ, Kvassman JO, Yunus S, Thompson JH, Betts RL, Lutter LC, and Shore JD (2003) Mutation of the highly conserved tryptophan in the serpin breach region alters the inhibitory mechanism of plasminogen activator inhibitor-1. *Biochemistry* **42:**12260–12272.

Bødker JS, Wind T, Jensen JK, Hansen M, Pedersen KE, and Andreasen PA (2003) Mapping of the epitope of a monoclonal antibody protecting plasminogen activator inhibitor-1 against inactivating agents. *Eur J Biochem* **270:**1672–1679.

Bryans J, Charlton P, Chicarelli-Robinson I, Collins M, Faint R, Latham C, Shaw I, and Trew S (1996) Inhibition of plasminogen activator inhibitor-1 activity by two diketopiperazines, XR330 and XR334 produced by Streptomyces sp. *J Antibiot (Tokyo)* **49:**1014–1021.

Charlton P, Faint R, Barnes C, Bent F, Folkes A, Templeton D, Mackie I, Machin S, and Bevan P (1997) XR5118, a novel modulator of plasminogen activator inhibitor-1 (PAI-1), increases endogenous tPA activity in the rat. *Fibrinolysis Proteolysis* **11:**51–56.

Charlton PA, Faint RW, Bent F, Bryans J, Chicarelli-Robinson I, Mackie I, Machin S, and Bevan P (1996) Evaluation of a low molecular weight modulator of human plasminogen activator inhibitor-1 activity. *Thromb Haemost* **75:**808–815.

Chikanishi T, Shinohara C, Kikuchi T, Endo A, and Hasumi K (1999) Inhibition of plasminogen activator inhibitor-1 by 11-keto-9(*E*),12(*E*)-octadecadienoic acid, a novel fatty acid produced by Trichoderma sp. *J Antibiot (Tokyo)* **52:**797–802.

Crandall DL, Elokdah H, Di L, Hennan JK, Gorlatova NV, and Lawrence DA (2004) Characterization and comparative evaluation of a structurally unique PAI-1 inhibitor exhibiting oral in-vivo efficacy. *J Thromb Haemost* **2:**1422–1428.

Declerck PJ, Verstreken M, and Collen D (1995) Immunoassay of murine t-PA, u-PA and PAI-1 using monoclonal antibodies raised in gene-inactivated mice. *Thromb Haemost* **74:**1305–1309.

De Nanteuil G, Lila-Ambroise C, Rupin A, Vallez MO, and Verbeuren TJ (2003) New

fibrinolytic agents: benzothiophene derivatives as inhibitors of the t-PA-PAI-1 complex formation. *Bioorg Med Chem Lett* **13:**1705–1708.

Dupont DM, Blouse GE, Hansen M, Mathiasen L, Kjelgaard S, Jensen JK, Christensen A, Gils A, Declerck PJ, Andreasen PA, et al. (2006) Evidence for a pre-latent form of the serpin plasminogen activator inhibitor-1 with a detached beta-strand 1C. *J Biol Chem* **281:**36071–36081.

Durand MK, Bødker JS, Christensen A, Dupont DM, Hansen M, Jensen JK, Kjelgaard S, Mathiasen L, Pedersen KE, Skeldal S, et al. (2004) Plasminogen activator inhibitor-I and tumour growth, invasion, and metastasis. *Thromb Haemost* **91:**438–449.

Egelund R, Einholm AP, Pedersen KE, Nielsen RW, Christensen A, Deinum J, and Andreasen PA (2001a) A regulatory hydrophobic area in the flexible joint region of plasminogen activator inhibitor-1, defined with fluorescent activity- neutralizing ligands. ligand-induced serpin polymerization. *J Biol Chem* **276:**13077–13086.

Egelund R, Petersen TE, and Andreasen PA (2001b) A serpin-induced extensive proteolytic susceptibility of urokinase-type plasminogen activator implicates distortion of the proteinase substrate-binding pocket and oxyanion hole in the serpin inhibitory mechanism. *Eur J Biochem* **268:**673–685.

Ehnebom J, Björquist P, Anderson J-O, Johansson T, and Deinum J (1997) Detergent Tween 80 modifies the specific activity of PAI-1. *Fibrinolysis Proteolysis* **11:**165–170.

Ehrlich HJ, Gebbink RK, Keijer J, and Pannekoek H (1992) Elucidation of structural requirements on plasminogen activator inhibitor 1 for binding to heparin. *J Biol Chem* **267:**11606–11611.

Einholm AP, Pedersen KE, Wind T, Kulig P, Overgaard MT, Jensen JK, Bødker JS, Christensen A, Charlton P, and Andreasen PA (2003) Biochemical mechanism of action of a diketopiperazine inactivator of plasminogen activator inhibitor-1. *Biochem J* **373:**723–732.

Eitzman DT, Fay WP, Lawrence DA, Francis-Chmura AM, Shore JD, Olson ST, and Ginsburg D (1995) Peptide-mediated inactivation of recombinant and platelet plasminogen activator inhibitor-1 in vitro. *J Clin Invest* **95:**2416–2420.

Folkes A, Roe MB, Sohal S, Golec J, Faint R, Brooks T, and Charlton P (2001) Synthesis and in vitro evaluation of a series of diketopiperazine inhibitors of plasminogen activator inhibitor-1. *Bioorg Med Chem Lett* **11:**2589–2592.

Friederich PW, Levi M, Biemond BJ, Charlton P, Templeton D, van Zonneveld AJ, Bevan P, Pannekoek H, and ten Cate JW (1997) Novel low-molecular-weight inhibitor of PAI-1 (XR5118) promotes endogenous fibrinolysis and reduces post-thrombolysis thrombus growth in rabbits. *Circulation* **96:**916–921.

Gårdsvoll H, van Zonneveld AJ, Holm A, Eldering E, van Meijer M, Danø K, and Pannekoek H (1998) Selection of peptides that bind to plasminogen activator inhibitor 1 (PAI-1) using random peptide phage-display libraries. *FEBS Lett* **431:**170–174.

Gils A and Declerck PJ (1998) Modulation of plasminogen activator inhibitor 1 by Triton X-100– identification of two consecutive conformational transitions. *Thromb Haemost* **80:**286–291.

Gils A and Declerck PJ (2004) The structural basis for the pathophysiological relevance of PAI-I in cardiovascular diseases and the development of potential PAI-I inhibitors. *Thromb Haemost* **91:**425–437.

Gils A, Knockaert I, Brouwers E, and Declerck PJ (2000) Glycosylation dependent conformational transitions in plasminogen activator inhibitor-1: evidence for the presence of two active conformations. *Fibrinolysis Proteolysis* **14:**58–64.

Gils A, Pedersen KE, Skottrup P, Christensen A, Naessens D, Deinum J, Enghild JJ, Declerck PJ, and Andreasen PA (2003) Biochemical importance of glycosylation of plasminogen activator inhibitor-1. *Thromb Haemost* **90:**206–217.

Gils A, Stassen JM, Nar H, Kley JT, Wienen W, Ries UJ, and Declerck PJ (2002) Characterization and comparative evaluation of a novel PAI-1 inhibitor. *Thromb Haemost* **88:**137–143.

Gorlatova NV, Cale JM, Elokdah H, Li D, Fan K, Warnock M, Crandall DL, and Lawrence DA (2007) Mechanism of inactivation of plasminogen activator inhibitor-1 by a small molecule inhibitor. *J Biol Chem* **282:**9288–9296.

Gorlatova NV, Elokdah H, Fan K, Crandall DL, and Lawrence DA (2003) Mapping of a conformational epitope on plasminogen activator inhibitor-1 by random mutagenesis. Implications for serpin function. *J Biol Chem* **278:**16329–16335.

Hansen M, Wind T, Blouse GE, Christensen A, Petersen HH, Kjelgaard S, Mathiasen L, Holtet TL, and Andreasen PA (2005) A urokinase-type plasminogen activator-inhibiting cyclic peptide with an unusual P2 residue and an extended protease binding surface demonstrates new modalities for enzyme inhibition. *J Biol Chem* **280:**38424–38437.

Huntington JA (2006) Shape-shifting serpins–advantages of a mobile mechanism. *Trends Biochem Sci* **31:**427–435.

Jensen JK, Malmendal A, Schiøtt B, Skeldal S, Pedersen KE, Celik L, Nielsen NC, Andreasen PA, and Wind T (2006) Inhibition of plasminogen activator inhibitor-1 binding to endocytosis receptors of the low-density-lipoprotein receptor family by a peptide isolated from a phage display library. *Biochem J* **399:**387–396.

Koivunen E, Wang B, and Ruoslahti E (1994) Isolation of a highly specific ligand for the α5β1 integrin from a phage display library. *J Cell Biol* **124:**373–380.

Kvassman JO and Shore JD (1995) *Fibrinolysis:*215–221.

Munch M, Heegaard C, Jensen PH, and Andreasen PA (1991) Type-1 inhibitor of plasminogen activators. Distinction between latent, activated and reactive centre-cleaved forms with thermal stability and monoclonal antibodies. *FEBS Lett* **295:**102–106.

Munch M, Heegaard CW, and Andreasen PA (1993) Interconversions between active, inert and substrate forms of denatured/refolded type-1 plasminogen activator inhibitor. *Biochim Biophys Acta* **1202:**29–37.

Naessens D, Gils A, Compernolle G, and Declerck PJ (2003) Elucidation of the epitope of a latency-inducing antibody: identification of a new molecular target for PAI-1 inhibition. *Thromb Haemost* **90:**52–58.

Neve J, Leone PA, Carroll AR, Moni RW, Paczkowski NJ, Pierens G, Björquist P, Deinum J, Ehnebom J, Inghardt T, et al. (1999) Sideroxylonal C, a new inhibitor of human plasminogen activator inhibitor type-1, from the flowers of Eucalyptus albens. *J Nat Prod* **62:**324–326.

Nielsen LS, Andreasen PA, Grøndahl-Hansen J, Huang JY, Kristensen P, and Danø K (1986) Monoclonal antibodies to human 54,000 molecular weight plasminogen activator inhibitor from fibrosarcoma cells–inhibitor neutralization and one-step affinity purification. *Thromb Haemost* **55:**206–212.

Offersen BV, Nielsen BS, Høyer-Hansen G, Rank F, Hamilton-Dutoit S, Overgaard J, and Andreasen PA (2003) The myofibroblast is the predominant plasminogen activator inhibitor-1-expressing cell type in human breast carcinomas. *Am J Pathol* **163:**1887–1899.

Pedersen KE, Einholm AP, Christensen A, Schack L, Wind T, Kenney JM, and Andreasen PA (2003) Plasminogen activator inhibitor-1 polymers, induced by inactivating amphipathic organochemical ligands. *Biochem J* **372:**747–755.

Schulze AJ, Baumann U, Jaeger E, Huber R, and Laurell CB (1990) Structural transition of alpha 1-antitrypsin by a peptide sequentially similar to beta-strand s4A. *Eur J Biochem* **194:**51–56.

Scott JK and Smith GP (1990) Searching for peptide ligands with an epitope library. *Science* **249:**386–390.

Shore JD, Day DE, Francis-Chmura AM, Verhamme I, Kvassman J, Lawrence DA, and Ginsburg D (1995) A fluorescent probe study of plasminogen activator inhibitor-1. Evidence for reactive center loop insertion and its role in the inhibitory mechanism. *J Biol Chem* **270:**5395–5398.

Stoppelli MP, Andersen LM, Votta G, and Andreasen PA (2008). Engineered antagonists of uPA and PAI-1. Springer, New York, in press.

Stout TJ, Graham H, Buckley DI, and Matthews DJ (2000) Structures of active and latent PAI-1: a possible stabilizing role for chloride ions. *Biochemistry* **39:**8460–8469.

Sumbayev VV, Bonefeld-Jørgensen EC, Wind T, and Andreasen PA (2005) A novel pesticide-induced conformational state of the oestrogen receptor ligand-binding domain, detected by conformation-specific peptide binding. *FEBS Lett* **579:**541–548.

Urano T, Strandberg L, Johansson LB, and Ny T (1992) A substrate-like form of plasminogen-activator-inhibitor type 1. Conversions between different forms by sodium dodecyl sulphate. *Eur J Biochem* **209:**985–992.

Vaughan DE (1998) Plasminogen activator inhibitor-1: a common denominator in cardiovascular disease. *J Investig Med* **46:**370–376.

Verhamme I, Kvassman JO, Day D, Debrock S, Vleugels N, Declerck PJ, and Shore JD (1999) Accelerated conversion of human plasminogen activator inhibitor-1 to its latent form by antibody binding. *J Biol Chem* **274:**17511–17517.

Wang S, Golec J, Miller W, Milutinovic S, Folkes A, Williams S, Brooks T, Hardman K, Charlton P, Wren S, et al. (2002) Novel inhibitors of plasminogen activator inhibitor-1: development of new templates from diketopiperazines. *Bioorg Med Chem Lett* **12:**2367–2370.

Wind T, Hansen M, Jensen JK, and Andreasen PA (2002) The molecular basis for anti-proteolytic and non-proteolytic functions of plasminogen activator inhibitor type-1. Roles of the reactive centre loop, the shutter region, the flexible joint-region and the small serpin fragment. *Biol Chem* **383:**21–36.

Wind T, Jensen JK, Dupont DM, Kulig P, and Andreasen PA (2003) Mutational analysis of plasminogen activator inhibitor-1. *Eur J Biochem* **270:**1680–1688.

Wind T, Jensen MA, and Andreasen PA (2001) Epitope mapping for four monoclonal antibodies against human plasminogen activator inhibitor type-1. Implications for antibody-mediated PAI-1-neutralization and vitronectin-binding. *Eur J Biochem* **268:**1095–1106.

Xue Y, Björquist P, Inghardt T, Linschoten M, Musil D, Sjölin L, and Deinum J (1998) Interfering with the inhibitory mechanism of serpins: crystal structure of a complex formed between cleaved plasminogen activator inhibitor type 1 and a reactive-centre loop peptide. *Structure* **6:**627–636.

Address correspondence to: Peter A. Andreasen, Laboratory of Cellular Protein Science, Department of Molecular Biology, Aarhus University, 10C Gustav Wied's Vej, 8000 Aarhus C, Denmark. E-mail: pa@mb.au.dk